GEOLOGY
E: geology@geosociety.org
W: geosociety.org/gsa
T: @geosociety

Reaction-induced embrittlement of the lower continental crust

Tracking no: G45527

Authors:
Sarah Incel (University of Oslo), Loic Labrousse (Université Pierre & Marie Curie - Paris 6), Nadege Hilairet (CNRS), Timm John (Freie Universität Berlin), Julien Gasc (Ecole Normale Supérieure Paris), Feng Shi (University of Chicago), Yanbin Wang (University of Chicago), Torgeir Andersen (University of Oslo), François Renard (University of Oslo), Bjørn Jamtveit (University of Oslo), and Alex Schubnel

Abstract:
Field observations and geophysical data reveal a causal link between brittle seismic failure and eclogitization of the lower continental crust. We present results from experimental deformation of plagioclase-rich samples at eclogite-facies conditions and quantify the link between rock rheology and the kinetics of the eclogitization reactions. The deformation was ductile both in the absence of reaction and when the progress of eclogitization was fast compared to the imposed strain rate. However, when the reaction rate was relatively slow, the breakdown of plagioclase into nanocrystalline reaction products induced a weakening that triggered seismic failure. Fluid-induced plagioclase breakdown under eclogite-facies conditions is an exothermic reaction accompanied by a negative change in solid volume. This is similar to other mineral transformations that are known to trigger transformational faulting. We demonstrate that mineral reactions lead to brittle deformation in situations where reaction rates are slow compared to the deformation rate. This reaction-induced instability may provide a generic mechanism for embrittlement at depths beyond the normal seismogenic zone.

Reaction-induced embrittlement of the lower continental crust

Sarah Incel[1,2], Loïc Labrousse[3], Nadège Hilairet[4], Timm John[5], Julien Gasc[2], Feng Shi[6], Yanbin Wang[6], Torgeir B. Andersen[7], François Renard[1,8], Bjørn Jamtveit[1], and Alexandre Schubnel[2]

[1]Physics of Geological Processes, The Njord Centre, Department of Geosciences, University of Oslo, Box 1048 Blindern, 0316 Oslo, Norway, s.h.m.incel@geo.uio.no, francois.renard@geo.uio.no, bjorn.jamtveit@geo.uio.no

[2]Laboratoire de Géologie de l'ENS - PSL Research University - UMR8538 du CNRS, 24 Rue Lhomond, 75005 Paris, France, gasc@geologie.ens.fr, aschubnel@geologie.ens.fr

[3]Sorbonne Université, CNRS-INSU, Institut des Sciences de la Terre Paris, ISTeP, UMR 7193, 75005 Paris, France, loic.labrousse@upmc.fr

[4]Univ. Lille, CNRS, INRA, ENSCL, UMR 8207 - Unité Matériaux et Transformations, 59000 Lille, France, nadege.hilairet@univ-lille1.fr

[5]Freie Universität Berlin, Institute of Geological Sciences, Malteserstr. 74-100, 12249 Berlin, Germany, timm.john@fu-berlin.de

[6]Center for Advanced Radiation Sources, the University of Chicago, Chicago, IL 60637, USA, shi@cars.uchicago.edu, wang@cars.uchicago.edu

[7]Centre for Earth Evolution and Dynamics, Department of Geosciences, University of Oslo, Box 1047, Blindern, 0316 Oslo, Norway, t.b.andersen@geo.uio.no

[8]Univ. Grenoble Alpes, Univ. Savoie Mont Blanc, CNRS, IRD, IFSTTAR, ISTerre, Grenoble, France

ABSTRACT

Field observations and geophysical data reveal a causal link between brittle seismic failure and eclogitization of the lower continental crust. We present results from experimental deformation of plagioclase-rich samples at eclogite-facies conditions and quantify the link between rock rheology and the kinetics of the eclogitization reactions. The deformation was ductile both in the absence of reaction and when the progress of eclogitization was fast compared to the imposed strain rate. However, when the reaction rate was relatively slow, the breakdown of plagioclase into nanocrystalline reaction products induced a weakening that triggered seismic failure. Fluid-induced plagioclase breakdown under eclogite-facies conditions is an exothermic reaction accompanied by a negative change in solid volume. This is similar to other mineral transformations that are known to trigger transformational faulting. We demonstrate that mineral reactions lead to brittle deformation in situations where reaction rates are slow compared to the deformation rate. This reaction-induced instability may provide a generic mechanism for embrittlement at depths beyond the normal seismogenic zone.

INTRODUCTION

The mechanisms leading to brittle seismic failure in Earth's lower continental crust are still poorly understood. On the one hand, experimental studies reveal that plastic deformation should be dominant in plagioclase-rich rocks under granulite-facies conditions (<1 GPa and 973 K; Tullis and Yund, 1992) in the presence of water (Bürgmann and Dresen, 2008). On the other hand, field studies on lower-crustal rocks in Norway and geophysical data of the Himalaya-Tibetan plateau reveal a strong coupling between seismicity, fluid infiltration, and eclogitization of the metastable lower continental crust (Austrheim and Boundy, 1994; Jackson et al., 2004; Lund et al., 2004; Hetényi et al., 2007; John et al., 2009; Jamtveit et al., 2018).

Here, we present an experimental study on the rheology of plagioclase-rich rocks under eclogite-facies conditions. We show that metamorphic reactions enable embrittlement and propose a model that can be scaled up to natural systems.

MATERIALS AND METHODS

A granulite from Holsnøy, SW Norway, was used as sample material. It mostly contained plagioclase (≈ 90 vol.%) and minor amounts of zoisite, sometimes intergrown with alkali feldspar, spinel, corundum, clinopyroxene, amphibole, biotite, kyanite, garnet, and magnetite that make up the remaining 10 vol.% (Fig. DR1 in the GSA Data Repository[1]). The sample was crushed and sieved to a grain size of <38 µm. This powder was washed using distilled water to remove the dust fraction, dried in an oven, and then left at air humidity conditions. The same starting material was used for all experimental runs. The deformation experiments were conducted using the D-DIA apparatus (Wang et al., 2003), a deformation multi-anvil press, at the GSECARS beamline 13 BM-D of the Advanced Photon Source, Argonne National Laboratory, IL, USA. The D-DIA is equipped with an acoustic emission setup. The experimental setup is explained in detailed in Gasc et al.(2011) and Schubnel et al.(2013). Synchrotron X-ray radiographs as well as powder diffraction patterns were acquired every five minutes, respectively, to monitor the strain and the differential stress of the sample during the experimental run, at in-situ *P*-*T* conditions. Experimental conditions are summarized in the table in Figure 1. Details on the stress and strain calculation as well as on the analytical methods are given in section DR1 and DR2 in the Data Repository.

RESULTS

Based on the comparison of the overall stress-strain evolution together with the record of acoustic emissions between the four experimental runs, three different mechanical behaviors can be distinguished. Differential stress continuously increases during the deformation of

sample NG_2.5_1023 (constant *T*), which exhibits the highest strength and the least detected number of acoustic emissions (Fig. DR2A, C in the Data Repository). We refer to this behavior as strong and ductile. For sample NG_2.5_1173 (constant *T*) the differential stress first increases to a peak stress of ~1.8 GPa at ~15 % axial strain and then remains approximately constant until the end of deformation. A total of 794 acoustic emissions are recorded during deformation, hence this sample is in the brittle regime. Samples NG_2.5_1225 and NG_3_1225 both exhibit stress increase to ~2.3 GPa, followed by a large stress drop at ~14 % axial strain. Their stress drop correlates with an imposed increase in temperature and does not coincide with the onset of acoustic emissions (dashed vertical lines in Fig. DR2 in the Data Repository). These samples show a large variation in the total number of acoustic emissions: 82 for sample NG_2.5_1225 and only 9 for NG_3_1225. Sample NG_2.5_1225 clearly shows ample evidence for brittle deformation while NG_3_1225 is weak and ductile (Fig. DR2A, C in the Data Repository). Figure 1 shows the calculated evolution in mean stress, $\sigma_m = (\sigma_1+2\sigma_3)/3$, with temperature. All samples are deformed under eclogite-facies conditions outside the plagioclase stability field (Fig. 1; De Capitani and Petrakakis, 2010). The samples deformed furthest from the plagioclase stability produce the least amount of acoustic emissions (Fig. 1).

Two main microstructural features appear in the samples after deformation. Backscattered electron (BSE) images show dark areas in the plagioclase matrix indicative of a local difference in chemical composition (Fig. 2A). Another feature is the appearance of bands that are brighter than the adjacent plagioclase matrix in BSE mode (Fig. 3G). Both features, the dark areas and the bright bands, are very small (often <1 μm) and seem to be composed of different phases (Fig. 2B; Fig. DR3D in the Data Repository). This makes precise measurements very difficult. However, energy-dispersive X-ray spectroscopy (EDS) analyses and semi-quantitative element distribution maps were acquired with the scanning electron

microscope (SEM) to compare the chemical composition between the plagioclase matrix and these features. The dark zones are enriched in Na and depleted in Ca relative to the plagioclase matrix, suggesting a chemical composition close to albite or jadeite (Fig. 2A). Those zones are prominent in sample NG_2.5_1173 and mostly contain nanocrystalline grains (Figs. DR3D, 4B in the Data Repository). The bright crystals that are most frequent in NG_3_1225 are mainly composed of elongated zoisite needles together with kyanite, quartz, and albite/jadeite (Fig. 2B, C). The location and abundance of both features within each sample are spatially correlated, but their respective amounts differ between samples (Fig. 3; Fig. DR3 in the Data Repository). The dark zones are prominent in sample NG_2.5_1173 (Fig. 2A) and rare in sample NG_3_1225 that mostly shows bright band-forming crystals (Figs. 2B). Sample NG_2.5_1225 shows both features in equal amounts (Fig. 3E, F).

DISCUSSION AND CONCLUSION

Both, the bright bands and the dark areas, reflect the onset of eclogitization by plagioclase breakdown in the presence of a hydrous fluid according to the reaction: plagioclase + fluid ↔ zoisite + kyanite + quartz ± $(NaSiCa_{-1}Al_{-1})_{plagioclase}$ ± jadeite (modified after Wayte et al., 1989). First, zoisite nucleates and grows followed by the other product phases, which start to nucleate and grow at a more advanced plagioclase-transformation stage of ~10 vol.% (Wayte et al., 1989). Reaction progress was estimated based on image analysis of the area fraction of the reaction products. Since kyanite and quartz are only found in sample NG_3_1225, this sample shows the highest degree of eclogitization, i.e. the highest reacted plagioclase volume, estimated to be ~10 vol.% (Wayte et al., 1989). With respect to NG_3_1225, the other samples show lower reacted plagioclase volumes of ~5 vol.% for NG_2.5_1225, ~2.5 vol.% for NG_2.5_1173, and less than 1 vol.% for NG_2.5_1023 (Fig. 3). It is likely that water from air humidity was adsorbed onto the grain surfaces during sample preparation, thus providing a possible fluid source to produce the hydrous phase zoisite. Another possible fluid source

could be plagioclase itself since it can contain minor amounts of water in its crystal structure. Although small amounts of fluid are available during deformation, the overall reaction kinetics is expected to be sluggish, because it involves two successive processes. On the one hand, plagioclase is highly metastable (Fig. 1) and its breakdown will occur very rapidly as soon as it gets in contact with even low amounts of water. On the other hand, the nucleation and growth of the reaction products is expected to be slower, because it involves chemical transport over longer distances. It is therefore reasonable to assume that the net rate of eclogitization is controlled by the nucleation and growth of the reaction products.

In a reacting rock, strain can be accommodated by transformation-induced volume changes. An imposed strain rate, $\dot{\varepsilon}$, can be expressed as the sum of a transformational strain rate, $\dot{\varepsilon}_t$, and a residual strain rate, $\dot{\varepsilon}_r$, with $\dot{\varepsilon} = \dot{\varepsilon}_t + \dot{\varepsilon}_r$. In this study, three scenarios can be deduced (Fig. 3): a) almost no reaction (NG_2.5_1023), b) slow net eclogitization (NG_2.5_1225 and NG_2.5_1173), and c) fast net eclogitization (NG_3_1225). If no or little deformation is accommodated by transformation reactions, the granulite is strong and ductile and the microstructure of the sample shows distributed microcracks (Fig. 3A, B), which trigger few acoustic emissions. If deformation can be partly accommodated by reaction and the net eclogitization is slow, the granulite samples show brittle behavior (Fig. 3C-F). Their microstructures contain partially eclogitized domains of nanocrystalline material (Figs. 2A; 3C-F). The residual strain, ε_r, concentrates in these zones, which are weaker than the host granulite, eventually leading to brittle failure accompanied by acoustic emissions. In contrast, when the net eclogitization is fast, the sample is weak and ductile (Fig. 3G, H). Its micro-and nanostructure demonstrates that it contains numerous eclogite-bands filled with oriented crystals (Figs. 2B-C), which enable sliding during further deformation. Because the mineral transformation kinetics depends on metastability (distance to equilibrium), plagioclase breakdown proceeds faster in sample NG_3_1225 than in sample NG_2.5_1225 deformed at a

lower confining pressure. In conclusion, embrittlement is triggered by plagioclase breakdown, but as eclogite formation progresses, the overall rheological behavior of the sample becomes controlled by the soft eclogite. This has also been observed on Holsnøy, where unreacted and undeformed strong granulite blocks are embedded within a matrix of weak and deformed eclogite (Austrheim, 1990).

Eclogitization in nature, e.g. on Holsnøy, took place at $\dot{\varepsilon}$ and T significantly lower than in our experiments. Assuming that the observed embrittlement is controlled solely by the rate of plagioclase breakdown relative to the imposed $\dot{\varepsilon}$, we can scale our laboratory conditions to those expected for natural systems. As a first order approximation, $\dot{\varepsilon}_t$ can be expressed as:

$$\dot{\varepsilon}_t = \Delta V/V \times (d/d_0)^2 \times k_0 \times exp^{-E_a/RT}. \quad (1)$$

This equation combines the volume change of the plagioclase breakdown reaction ($\Delta V/V$), the grain size dependence on transformation progress where d_0 is the initial grain size and d the grain size after a certain amount of reaction with an Arrhenius-type T-dependence of the transformation rate ($k_0 \times exp^{-E_a/RT}$). The parameters k_0, E_a, and R are the reaction rate constant, the activation energy, and the gas constant, respectively (see section DR1 for further details on the calculation of E_a). Assuming that the reaction extent required to cause embrittlement in the laboratory is similar in nature, the laboratory transformational strain rate, $\dot{\varepsilon}_{t,lab}$, and the natural transformational strain rates, $\dot{\varepsilon}_{t,nat}$, are related by:

$$\dot{\varepsilon}_{t,lab}/\dot{\varepsilon}_{t,nat} = \left(d_{0,nat}/d_{0,lab}\right)^2 \times exp\left(E_a/R \times (1/T_{nat} - 1/T_{lab})\right) \quad (2)$$

where T_{nat} is the eclogitization temperature on Holsnøy (~973 K; Raimbourg et al., 2005), and T_{lab} the temperature under which embrittlement is observed in our experiments (~1,173 K). The initial natural grain size $d_{0,nat}$ is ~1 to 3×10^{-3} m and the initial laboratory grain size $d_{0,lab}$ ~1 to 38×10^{-6} m. Figure 4 shows how the transformational strain rate ratio ($\dot{\varepsilon}_{t,lab}/\dot{\varepsilon}_{t,nat}$) required to cause brittle behavior varies with T. The onset of embrittlement would be expected at imposed natural strain rates $\dot{\varepsilon}_{nat}$~$10^{-9.8}$ s^{-1} (horizontal solid red line in

Fig. 4), if the grain size ratio is minimal $\left(d_{0,nat}/d_{0,lab}\right)^2_{min}$ (solid black line in Fig. 4). However, assuming a maximal initial grain size ratio $\left(d_{0,nat}/d_{0,lab}\right)^2_{max}$ (dashed black line in Fig. 4) yields even lower imposed natural strain rates of $\dot{\varepsilon}_{nat}$~$10^{-13.8}$ s^{-1} (horizontal dashed red line in Fig. 4).

Previous experiments on the Ge-olivine-spinel transition (Burnley et al., 1991) show a change in rheology similar to what is presented in this study. Both transformations, plagioclase breakdown and olivine-spinel transition (Kirby et al., 1996), involve a negative volume change of ~14-17 % and 3-10 % and an exothermic latent heat release of ~10-13 $kJ \cdot mol^{-1}$ and 10-50 $kJ \cdot mol^{-1}$, respectively. These thermodynamic properties probably play an important role in triggering brittle instabilities, as the negative volume change enables stress concentrations at crack tips (Kirby, 1987). Along with the heat released during the exothermic reactions, which would promote reactions to proceed even in the absence of larger amounts of fluid, these key ingredients may lead to the generation of self-localizing transformational faults. We show that, contrarily to what was previously argued (Kirby et al., 1996), transformational faulting is not limited to the case of polymorphic reactions.

Our results demonstrate that reaction-induced grain size reduction together with a negative volume change trigger embrittlement in the laboratory. This is in accordance with findings of previous numerical and experimental studies on various lithologies (Burnley et al., 1991; Thielmann et al., 2015; Incel et al., 2017) and highlights embrittlement in the lower continental crust, at intermediate depth or deep in Earth's mantle by the same underlying mechanism. It should be noted however, that the reaction-driven embrittlement mechanism studied here requires a local fluid source. Otherwise, there will be no reaction. In our experiments, there is a small amount of fluid available for hydration reactions. For the Holsnøy case, fluids are introduced to an initially dry lower crust by lower crustal earthquakes. Earthquakes in the lower crust prior to hydration may be triggered through stress

197 pulses from earthquakes in the normal seismogenic regime (i.e. as aftershocks, Jamtveit et al.
198 2018). Incipient eclogitization reactions would then allow further brittle deformation in the
199 wall rocks of earthquake generated faults. In the case of the subducting Indian lower crust,
200 deep crustal earthquakes have been interpreted to have been triggered by dehydration-
201 produced fluids derived from the crust itself (Hetényi et al., 2007), in which case, reaction-
202 driven embrittlement may even explain the initial earthquake activity.

ACKNOWLEDGEMENTS

The authors thank Damien Deldicque for the micro- and nanostructural analyses. The study received funding from the Alexander von Humboldt-foundation (Feodor Lynen-fellowship to SI). Further funding came from the People Program (Marie Curie Actions) of the European Union's Seventh Framework Program FP7/2017-2013/ and Horizon 2020 under REA grant agreements n° 604713 (to AS) and n° 669972 (to BJ), NRF-CoE-grant 223272 (TBA), EAR-1661489 for the development of AE experiments (YW). This research used resources of the Advanced Photon Source, a U.S. Department of Energy Office of Science User Facility operated by Argonne National Laboratory (contract n° DE-AC02-06CH11357).

REFERENCES CITED

Austrheim, H., 1990, The granulite-eclogite facies transition: A comparison of experimental work and a natural occurrence in the Bergen Arcs, western Norway: Lithos, v. 25, p. 163–169, doi: 10.1016/0024-4937(90)90012-P.

Austrheim, H., and Boundy, T.M., 1994, Pseudotachylytes Generated During Seismic Faulting and Eclogitization of the Deep Crust: Science, v. 265, p. 82–83, doi: 10.1126/science.265.5168.82.

Bürgmann, R., and Dresen, G., 2008, Rheology of the Lower Crust and Upper Mantle: Evidence from Rock Mechanics, Geodesy, and Field Observations: Annual Review of Earth and Planetary Sciences, v. 36, p. 531–567, doi: 10.1146/annurev.earth.36.031207.124326.

Burnley, P.C., Green, H.W., and Prior, D.J., 1991, Faulting associated with the olivine to spinel transformation in Mg 2 GeO 4 and its implications for deep-focus earthquakes: Journal of Geophysical Research, v. 96, p. 425–443, doi: 10.1029/90JB01937.

De Capitani, C., and Petrakakis, K., 2010, The computation of equilibrium assemblage diagrams with Theriak/Domino software: American Mineralogist, v. 95, p. 1006–1016, doi: 10.2138/am.2010.3354.

Gasc, J., Schubnel, A., Brunet, F., Guillon, S., Mueller, H.J., and Lathe, C., 2011, Simultaneous acoustic emissions monitoring and synchrotron X-ray diffraction at high pressure and temperature: Calibration and application to serpentinite dehydration: Physics of the Earth and Planetary Interiors, v. 189, p. 121–133, doi: 10.1016/j.pepi.2011.08.003.

Hetényi, G., Cattin, R., Brunet, F., Bollinger, L., Vergne, J., Nábělek, J.L., and Diament, M., 2007, Density distribution of the India plate beneath the Tibetan plateau: Geophysical and petrological constraints on the kinetics of lower-crustal eclogitization: Earth and Planetary Science Letters, v. 264, p. 226–244, doi: 10.1016/j.epsl.2007.09.036.

Incel, S., Hilairet, N., Labrousse, L., John, T., Deldicque, D., Ferrand, T.P., Wang, Y., Morales, L., and Schubnel, A., 2017, Laboratory earthquakes triggered during eclogitization of lawsonite-bearing blueschist: Earth and Planetary Science Letters, v. 459, p. 320–331, doi: 10.1016/j.epsl.2016.11.047.

Jackson, J.A., Austrheim, H., McKenzie, D., and Priestley, K., 2004, Metastability, mechanical strength, and the support of mountain belts: Geology, v. 32, p. 625–628, doi: 10.1130/G20397.1.

Jamtveit, B., Ben-Zion, Y., Renard, F., and Austrheim, H., 2018, Earthquake-induced transformation of the lower crust: Nature, v. 556, p. 487–491.

John, T., Medvedev, S., Rüpke, L.H., Andersen, T.B., Podladchikov, Y.Y., and Austrheim, H., 2009, Generation of intermediate-depth earthquakes by self-localizing thermal runaway: Nature Geoscience, v. 2, p. 137–140, doi: 10.1038/ngeo419.

Kirby, S.H., 1987, Localized polymorphic phase transformations in high-pressure faults and applications to the physical mechanism of deep earthquakes: Journal of Geophysical Research: Solid Earth, v. 92, p. 13789–13800, doi: 10.1029/JB092iB13p13789.

Kirby, S.H., Stein, S., Okal, E.A., and Rubie, D.C., 1996, Metastable mantle phase

transformations and deep earthquakes in subducting oceanic lithosphere: Reviews of Geophysics, v. 34, p. 261–306.

Lund, M.G., Austrheim, H., and Erambert, M., 2004, Earthquakes in the deep continental crust- insights from studies on exhumed high-pressure rocks: Geophysical Journal International, v. 158, p. 569–576.

Raimbourg, H., Jolivet, L., Labrousse, L., Leroy, Y., and Avigad, D., 2005, Kinematics of syneclogite deformation in the Bergen Arcs, Norway: implications for exhumation mechanisms: Geological Society, London, Special Publications, v. 243, p. 175–192, doi: 10.1144/GSL.SP.2005.243.01.13.

Schubnel, A., Brunet, F., Hilairet, N., Gasc, J., Wang, Y., and Green, H.W., 2013, Deep-focus earthquake analogs recorded at high pressure and temperature in the laboratory: Science, v. 341, p. 1377–1380, doi: 10.1126/science.1240206.

Thielmann, M., Rozel, A., Kaus, B.J.P., and Ricard, Y., 2015, Intermediate-depth earthquake generation and shear zone formation caused by grain size reduction and shear heating: Geology, v. 43, p. 791–794, doi: 10.1130/G36864.1.

Tullis, J., and Yund, R., 1992, The Brittle-Ductile Transition in Feldspar Aggregates: An Experimental Study: International Geophysics, v. 51, p. 89–117, doi: 10.1016/S0074-6142(08)62816-8.

Wang, Y., Durham, W.B., Getting, I.C., and Weidner, D.J., 2003, The deformation-DIA: A new apparatus for high temperature triaxial deformation to pressures up to 15 GPa: Review of Scientific Instruments, v. 74, p. 3002–3011, doi: 10.1063/1.1570948.

Wayte, G.J., Worden, R.H., Rubie, D.C., and Droop, G.T.R., 1989, A TEM study of disequilibrium plagioclase breakdown at high pressure: the role of infiltrating fluid: Contributions to Mineralogy and Petrology, v. 101, p. 426–437, doi: 10.1007/BF00372216.

[1]GSA Data Repository item 201Xxxx, details on the stress and strain calculation (DR1), the analytical methods (DR2), and the activation energy calculation (DR3), as well as Figs. DR1-5 is available online at www.geosociety.org/pubs/ft20XX.htm, or on request from editing@geosociety.org or Documents Secretary, GSA, P.O. Box 9140, Boulder, CO 80301, USA.

FIGURES

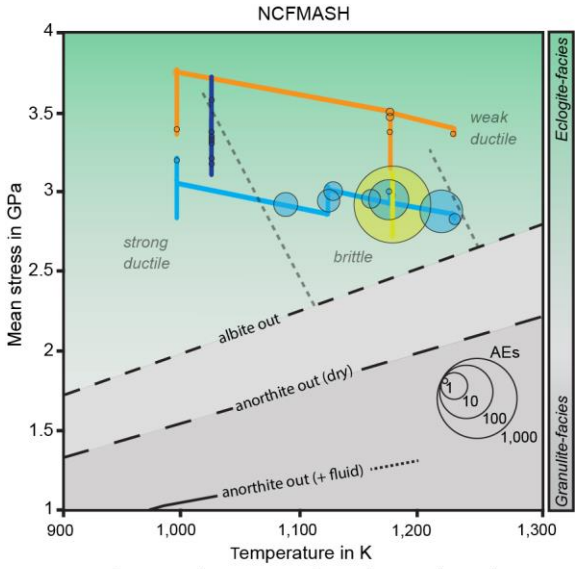

Sample	P_c in GPa	T in K	ε in %	$\dot{\varepsilon}$ in s^{-1}	# AEs	X in vol.%
NG_2.5_1023	2.5	1,023±50	35	5×10^{-5}	7	<1
NG_2.5_1173	2.5	1,173±50	37	6×10^{-5}	794	2.5
NG_2.5_1225	2.5	(995-1,225)±50	34	5×10^{-5}	82	5
NG_3_1225	3	(995-1,225)±50	36	5×10^{-5}	9	10

Figure 1: Mean stress-T curves on a P-T phase diagram showing the stability of plagioclase and the experimental conditions (table). P_c= confining pressure; T= temperature; ε= finite strain; $\dot{\boldsymbol{\varepsilon}}$= strain rate; X= reacted plagioclase volume. AEs: acoustic emissions.

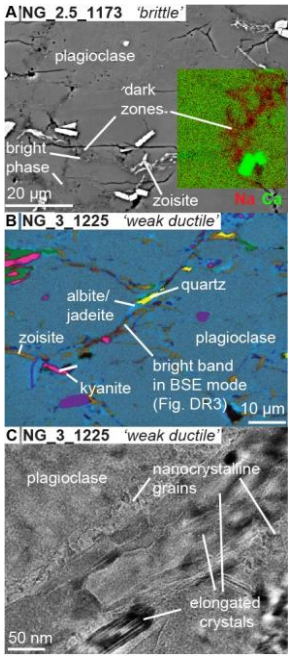

Figure 2: A) BSE image with superimposed composite EDS elemental map showing Ca and Na distribution. B) Composite EDS elemental map of the area marked in Figure DR3H. Bright bands in the microstructure are composed of zoisite + kyanite + quartz ± albite ±

jadeite. C) TEM image, taken in bright field mode, showing a cross-sectional view of a selected bright band composed of elongated crystals with borders of isometrically shaped crystals. The location of this image is shown in Fig. DR5 in the Data Repository. Maximum stress is vertical on images A) and B).

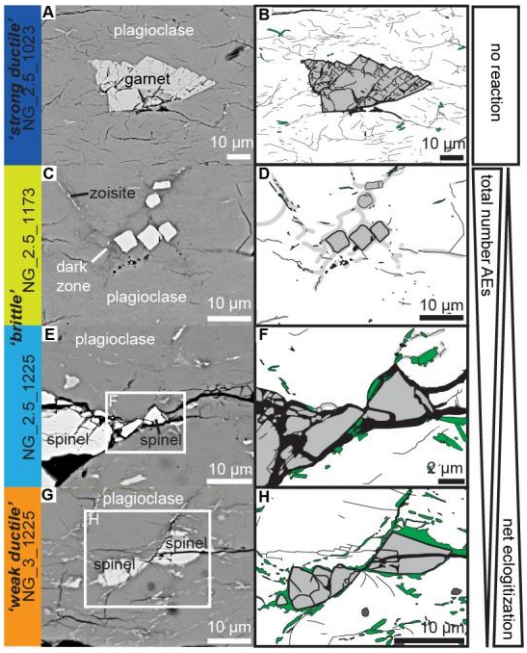

Figure 3: BSE images of the four samples (A, C, E, G) with corresponding sketches (B, D, F, H). Maximum stress is vertical. Net eclogitization is deduced from the abundance of eclogite-facies minerals with zoisite as a proxy (green areas in B, D, F, H). NG_2.5_1023 shows almost no reaction and is strong and ductile (A, B). Sample NG_2.5_1173 shows a low net eclogitization rate and is brittle (C, D). Although the net eclogitization rate in sample NG_2.5_1225 is higher compared to sample NG_2.5_1173, this sample is also brittle (E, F), because the amount of soft eclogite is not sufficient to dominate the overall rheological behavior. Sample NG_3_1225 shows weak and ductile behavior and its net eclogitization rate is high (G, H).

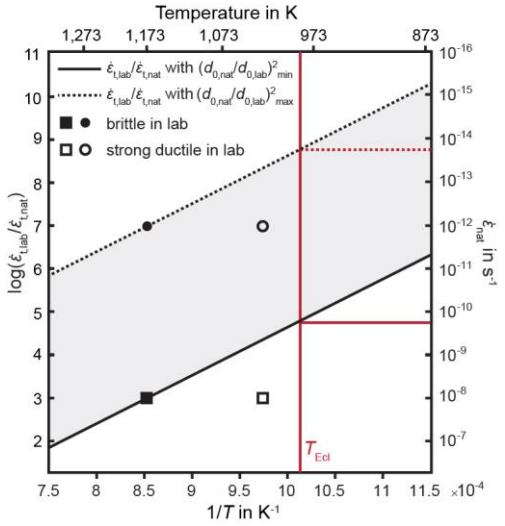

312

313 Figure 4: Arrhenius plot showing $\boldsymbol{log}(\dot{\varepsilon}_{t,lab}/\dot{\varepsilon}_{t,nat})$ versus 1/T. The red vertical line represents
314 the estimated eclogitization temperature on Holsnøy (T_{Ecl}). Depending on the initial grain size
315 ratio $d_{0,\mathrm{nat}}/d_{0,\mathrm{lab}}$ the required imposed natural strain rate ($\dot{\boldsymbol{\varepsilon}}_{\boldsymbol{nat}}$) for embrittlement is ~$10^{-9.8}$ to
316 $10^{-13.8}$ s^{-1} (solid and dashed red horizontal lines).

NGFMASH

Figure 1

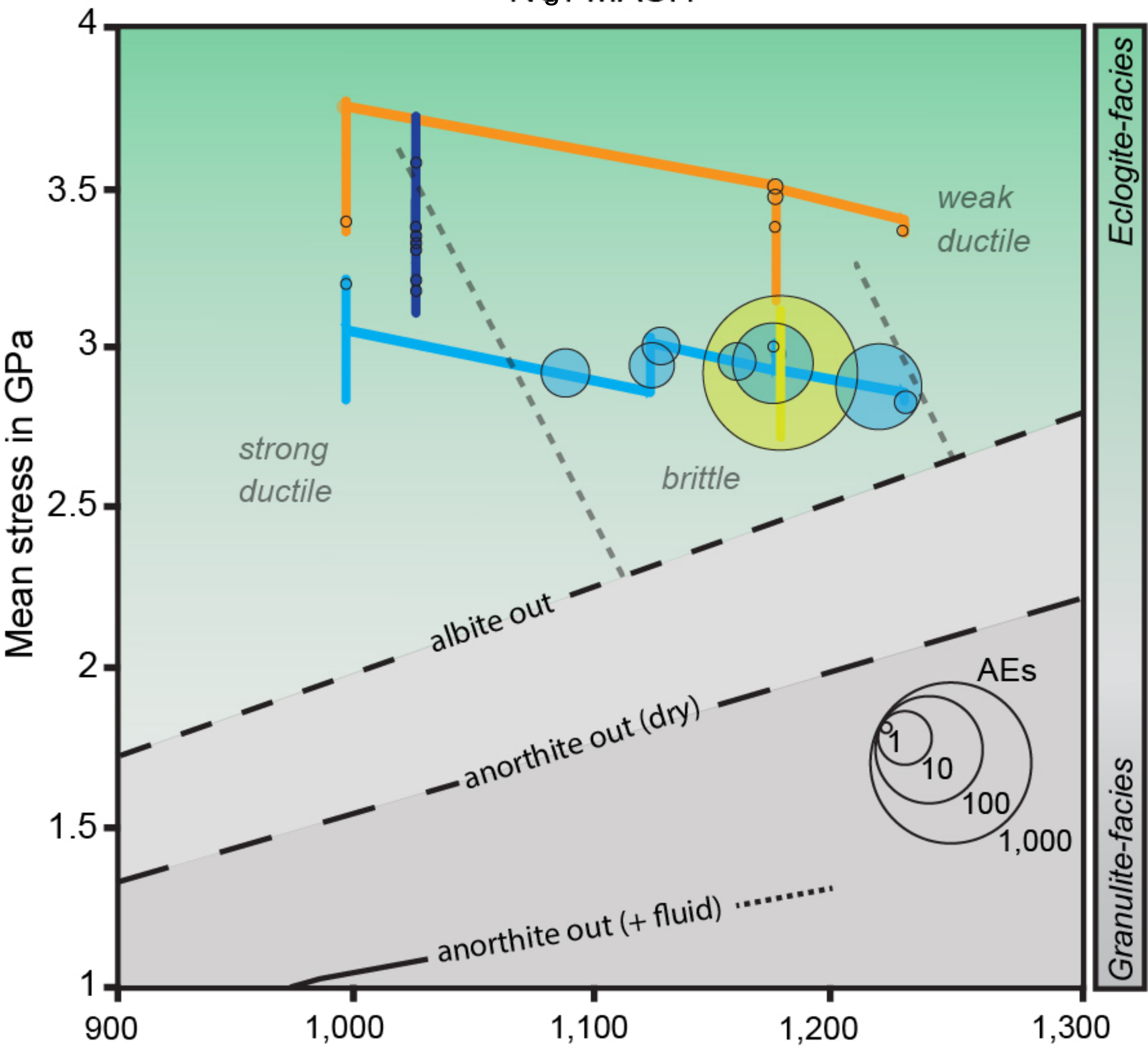

Sample	P_c in GPa	T in K	ε in %	$\dot{\varepsilon}$ in s^{-1}	# AEs	X in vol.%
NG_2.5_1023	2.5	1,023±50	35	5×10^{-5}	7	<1
NG_2.5_1173	2.5	1,173±50	37	6×10^{-5}	794	2.5
NG_2.5_1225	2.5	(995-1,225)±50	34	5×10^{-5}	82	5
NG_3_1225	3	(995-1,225)±50	36	5×10^{-5}	9	10

Figure 2

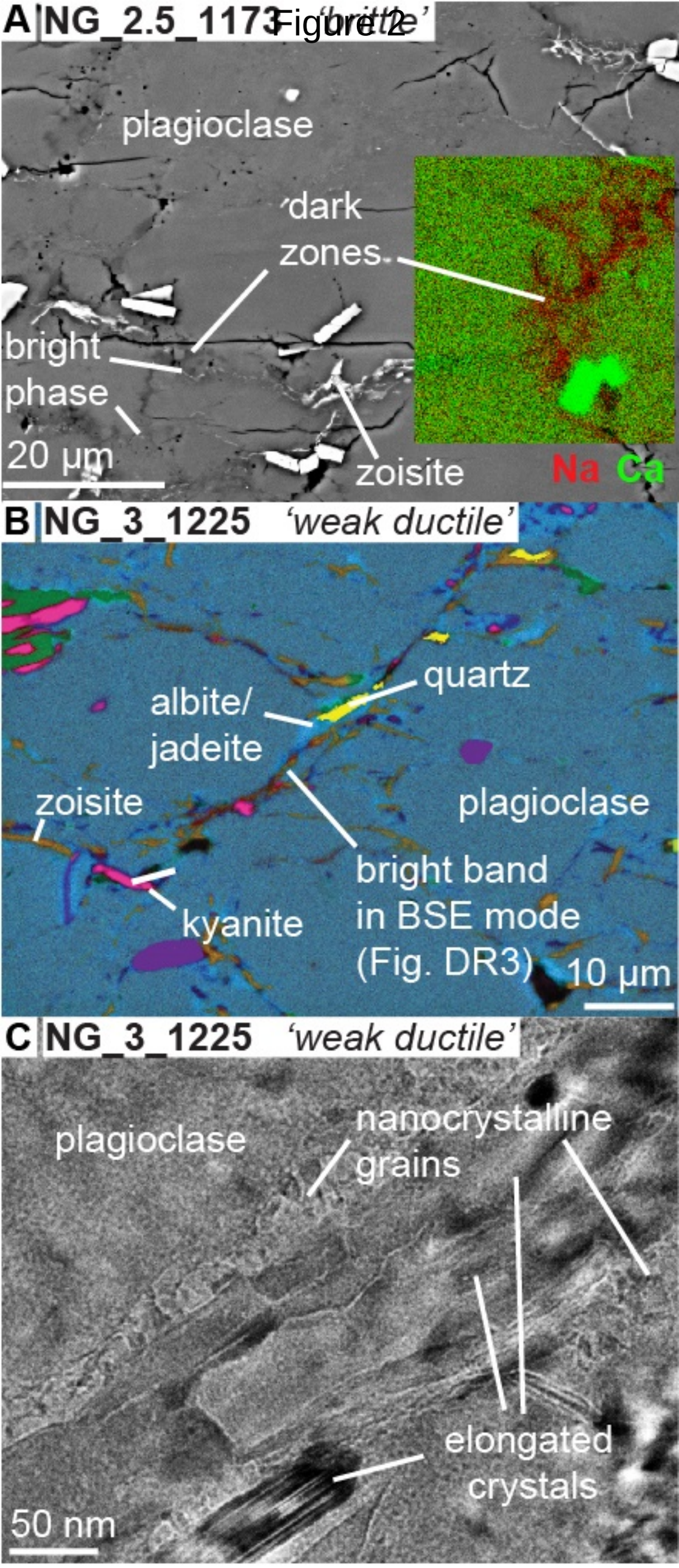
A NG_2.5_1173 'brittle'
plagioclase
dark zones
bright phase
20 µm
zoisite
Na Ca
B NG_3_1225 'weak ductile'
quartz
albite/ jadeite
zoisite
plagioclase
bright band in BSE mode (Fig. DR3)
kyanite
10 µm
C NG_3_1225 'weak ductile'
plagioclase
nanocrystalline grains
elongated crystals
50 nm

no reaction

net eclogitization

total number AEs

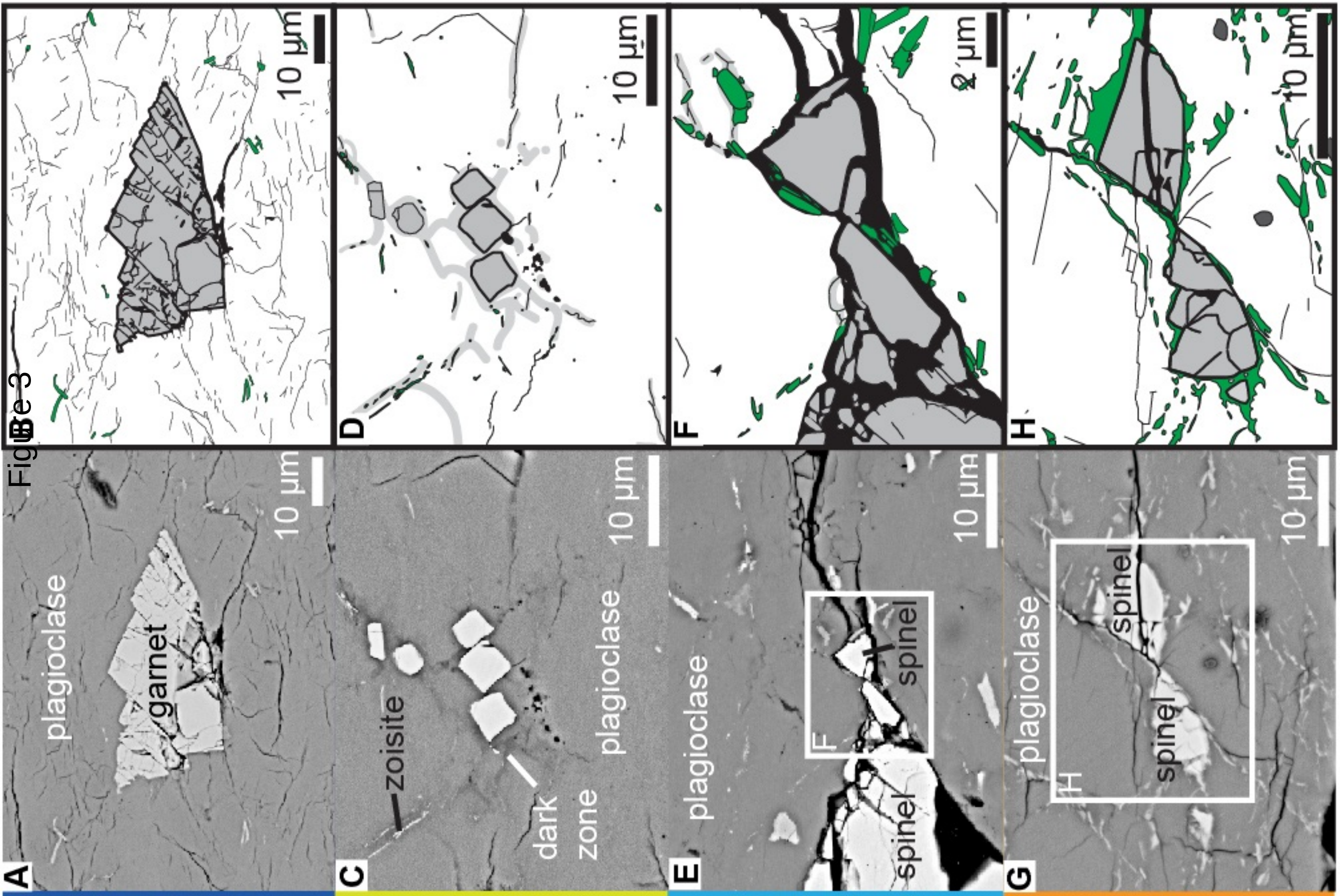

'strong ductile'
NG_2.5_1023

'brittle'
NG_2.5_1173

NG_2.5_1225

'weak ductile'
NG_3_1225

Fig. 3

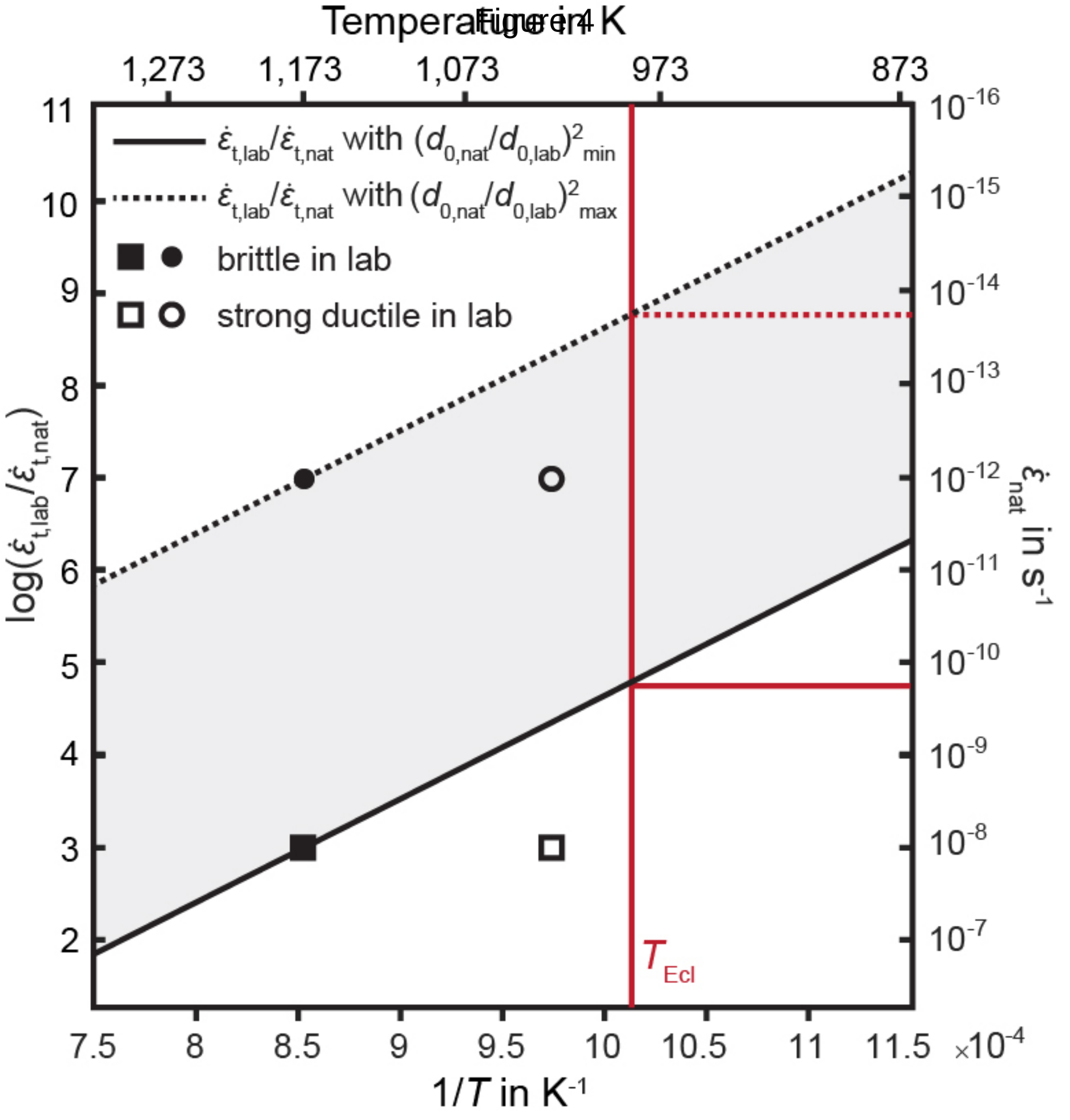
Temperature in K
1,273
1,173
1,073
973
873
$\dot{\varepsilon}_{t,lab}/\dot{\varepsilon}_{t,nat}$ with $(d_{0,nat}/d_{0,lab})^2_{min}$
$\dot{\varepsilon}_{t,lab}/\dot{\varepsilon}_{t,nat}$ with $(d_{0,nat}/d_{0,lab})^2_{max}$
brittle in lab
strong ductile in lab
T_{Ecl}
$\log(\dot{\varepsilon}_{t,lab}/\dot{\varepsilon}_{t,nat})$
$\dot{\varepsilon}_{nat}$ in s^{-1}
$1/T$ in K^{-1}
$\times 10^{-4}$

Data Repository for: Reaction-induced embrittlement of the lower continental crust

1 STRESS AND STRAIN CALCULATION

To monitor the strain during deformation gold foils that acted as strain markers in X-ray radiographs were placed at the bottom and the top of the sample. The powder diffraction patterns gave access to the differential stresses sustained by lattice planes of a certain phase due to the distortion of the Debye rings in an anisotropic stress field. Hilairet et al., (2012) give further details on the strain and stress calculation. These differential stresses were calculated on the (-201), (111), (002), and the (-220) lattice planes of plagioclase using available elasticity data (Brown et al., 2006) and thermal expansion coefficients (Tribaudino et al., 2010) from literature. The mean stresses of each experiment were re-calculated using the average of the differential stress on the (002) and the (111) lattice planes of plagioclase and the confining pressure (P_c). The confining pressures (see the table in Fig. 1) were estimated using the peak shift in the diffraction pattern taken at ambient conditions and after pressurization and heating. Because calculating stress using triclinic symmetry did not lead to reliable results, the calculation was performed with orthorhombic crystal symmetry. Prior to deformation, the powder samples were hot-pressed in-situ, at their respective confining pressures and their minimum temperatures (table in Fig. 1). After hot-pressing the samples for around one hour, deformation started at a controlled constant strain rate of $\sim 5 \cdot 10^{-5}$ s^{-1}.

2 ANALYTICAL METHODS

All samples were investigated using the Zeiss Sigma field-emission scanning electron microscope (FE-SEM) at Ecole Normale Supérieure, Paris. Backscattered electron (BSE) images were acquired with an acceleration voltage of 15 kV. For the energy-dispersive X-ray

spectroscopy (EDS) element distribution maps, the acceleration voltage was lowered to 10 kV to obtain a higher resolution. The electron backscatter diffraction (EBSD) analyses were performed using an Oxford instruments EBSD detector installed on the same SEM at Ecole Normale Supérieure Paris. Analyses were conducted at an acceleration voltage of 15 kV and the EBSD data was generated using the Oxford Instruments AZtecHKL EBSD system. To investigate the nanostructure, a focused ion beam (FIB) section was cut using a FEI Strata DB 235 at IEMN at the University of Lille, France. The transmission electron microscopy (TEM) analyses were performed on a JEM 2011 at the Laboratoire de Réactivité de Surface at Université Pierre et Marie Curie Paris, France. The TEM images were taken in bright field (BF) mode with an acceleration voltage of 200 kV.

3 CALCULATION OF E_a (EXPLANATIONS TO FIGURE 4)

To calculate the activation energy E_a, an Avrami type equation (Poirier, 1982)

$$X(t) = 1 - \exp(-kt^n) \quad (1)$$

was used, with X, the advancement of reaction, t, the time in seconds, and k the kinetics factor that can be written as an Arrhenius function

$$k = k_0 \times \exp(-E_a/RT), \quad (2)$$

where E_a is the activation energy term, R the gas constant and T the temperature in K. Assuming n=1 for nucleation at grain boundaries (Cahn, 1956), equations (1) and (2) derive into:

$$ln(X(t)) = k_0 \times \exp(-E_a/RT) \times t. \quad (3)$$

where X is the reacted granulite volume over t the finite duration of the experiments and is measured from microstructural observations. Considering that dX/dt, the instantaneous reaction rate is constant over the short duration of our experiments yields:

$$ln(X/(1-X))/t = k_0 \times \exp(-E_a/RT), \quad (4)$$

For the two experiments performed at constant temperature, NG_2.5_1023 and NG_2.5_1173, we plotted ln k_0 over 1/(RT). The slope of the regression line between these two points is the activation energy with $E_a \approx 215$ kJ·mol^{-1}. However, the reacted volumes cannot be estimated precisely and any change would affect the slope. The exact determination of E_a for anorthite breakdown in the presence of fluid exceeds the scope of the present study and since it lies in the same order of magnitude as E_a for other known transitions, e.g. 162 kJ·mol^{-1} for the quartz-coesite (Perrillat et al., 2003) and 259 kJ·mol^{-1} for the olivine-spinel transition (Poirier, 1981), we consider that for our purpose the calculated E_a represents a reasonable estimate of the activation energy.

Brown, J.M., Abramson, E.H., and Angel, R.J., 2006, Triclinic elastic constants for low albite: Physics and Chemistry of Minerals, v. 33, p. 256–265, doi: 10.1007/s00269-006-0074-1.

Cahn, J.W., 1956, The kinetics of grain boundary nucleated reactions: Acta Metallurgica, v. 4, p. 449–459, doi: 10.1016/0001-6160(56)90041-4.

Hilairet, N., Wang, Y., Sanehira, T., Merkel, S., and Mei, S., 2012, Deformation of olivine under mantle conditions: An in situ high-pressure, high-temperature study using monochromatic synchrotron radiation: Journal of Geophysical Research: Solid Earth, v. 117, p. 1–16, doi: 10.1029/2011JB008498.

Perrillat, J.P., Daniel, I., Lardeaux, J.M., and Cardon, H., 2003, Kinetics of the Coesite–Quartz Transition: Application to the Exhumation of Ultrahigh-Pressure Rocks: Journal of Petrology, v. 44, p. 773–788, doi: 10.1093/petrology/44.4.773.

Poirier, J.P., 1981, On the kinetics of olivine-spinel transition: Physics of the Earth and Planetary Interiors, v. 26, p. 179–187, doi: 10.1016/0031-9201(81)90006-6.

Poirier, J.P., 1982, On transformation plasticity: Journal of Geophysical Research, v. 87, p. 6791–6797.

Tribaudino, M., Angel, R.J., Cámara, F., Nestola, F., Pasqual, D., and Margiolaki, I., 2010, Thermal expansion of plagioclase feldspars: Contributions to Mineralogy and Petrology, v. 160, p. 899–908, doi: 10.1007/s00410-010-0513-3.

SUPPLEMENTARY FIGURES

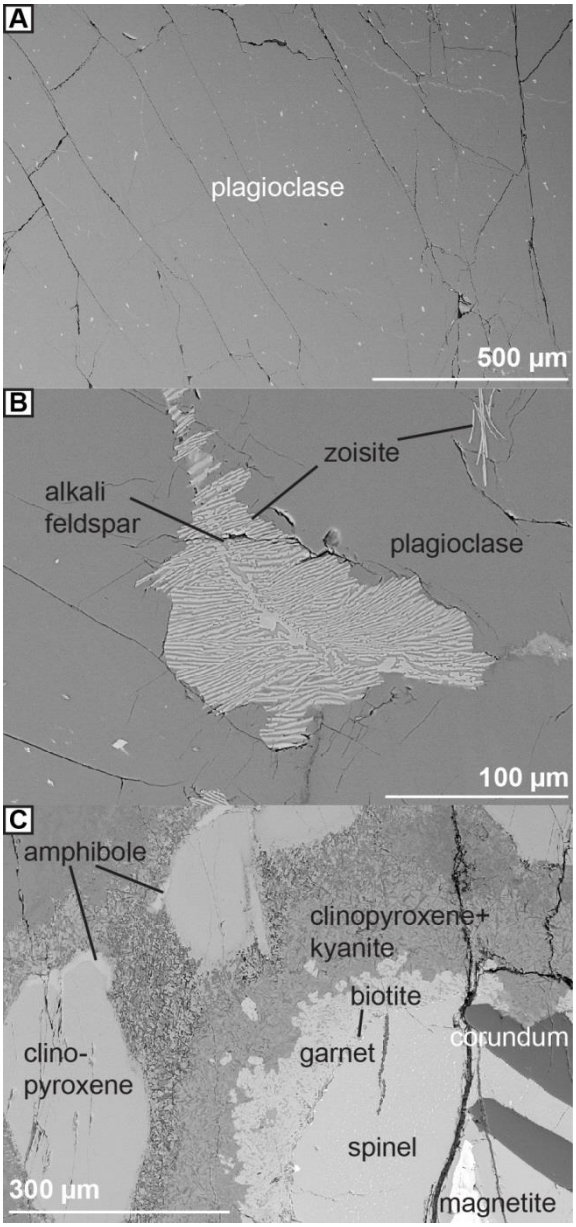

Fig. DR1: Backscattered electron images of the starting material. A) Most of the unaltered granulite consists of plagioclase showing intermediate composition ($An_{0.52}Ab_{0.46}Or_{0.02}$). B) Zoisite crystals in the plagioclase matrix and zoisite-alkali feldspar symplectites. C) Clinopyroxene, with areas showing amphibole composition, and spinel crystals, intergrown with corundum and magnetite, demonstrate mineralogically complex coronas composed of garnet, biotite, clinopyroxene, and kyanite needles.

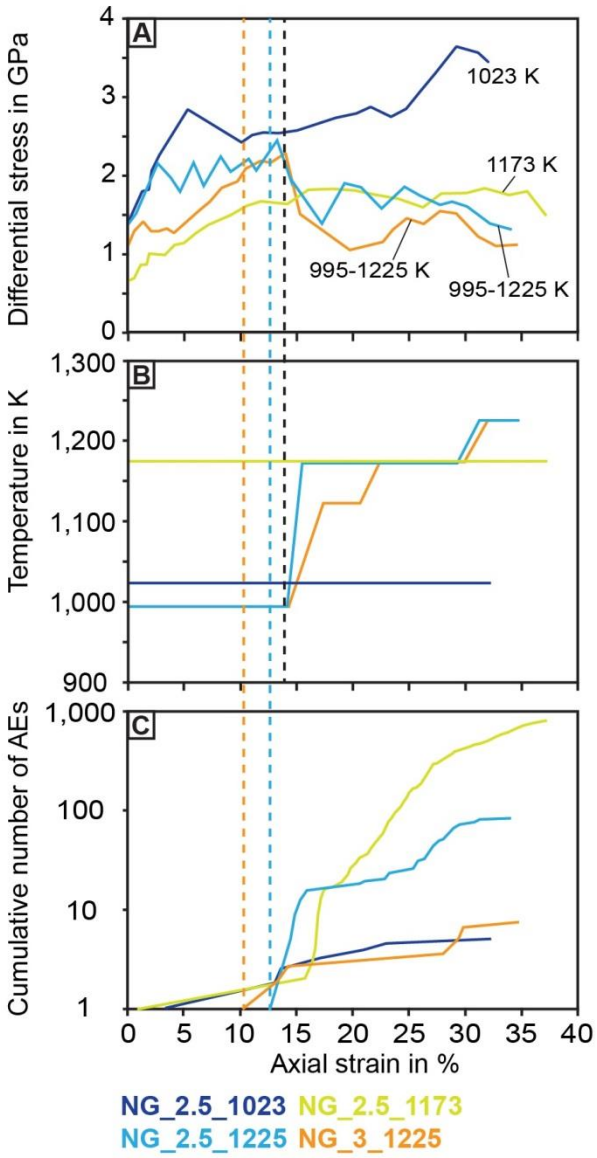

Fig. DR2: Differential stress-strain curves, temperature evolution, and record of acoustic emissions (AEs). a) Differential stress versus axial strain. The stress drops in the experiments NG_2.5_1225 (solid light blue curve) and NG_3_1225 (solid orange curve) coincide with the imposed temperature increase shown in B) (dashed black line). B) The temperature versus axial strain plot exhibits the temperature evolution of each sample during deformation. C) The cumulative number of AEs versus axial strain plot shows that a variable number of AEs were recorded during deformation of each run. The stress drops in A) do not correlate with the onset of AEs during deformation of NG_2.5_1225 and NG_3_1225 (dashed light blue and orange lines).

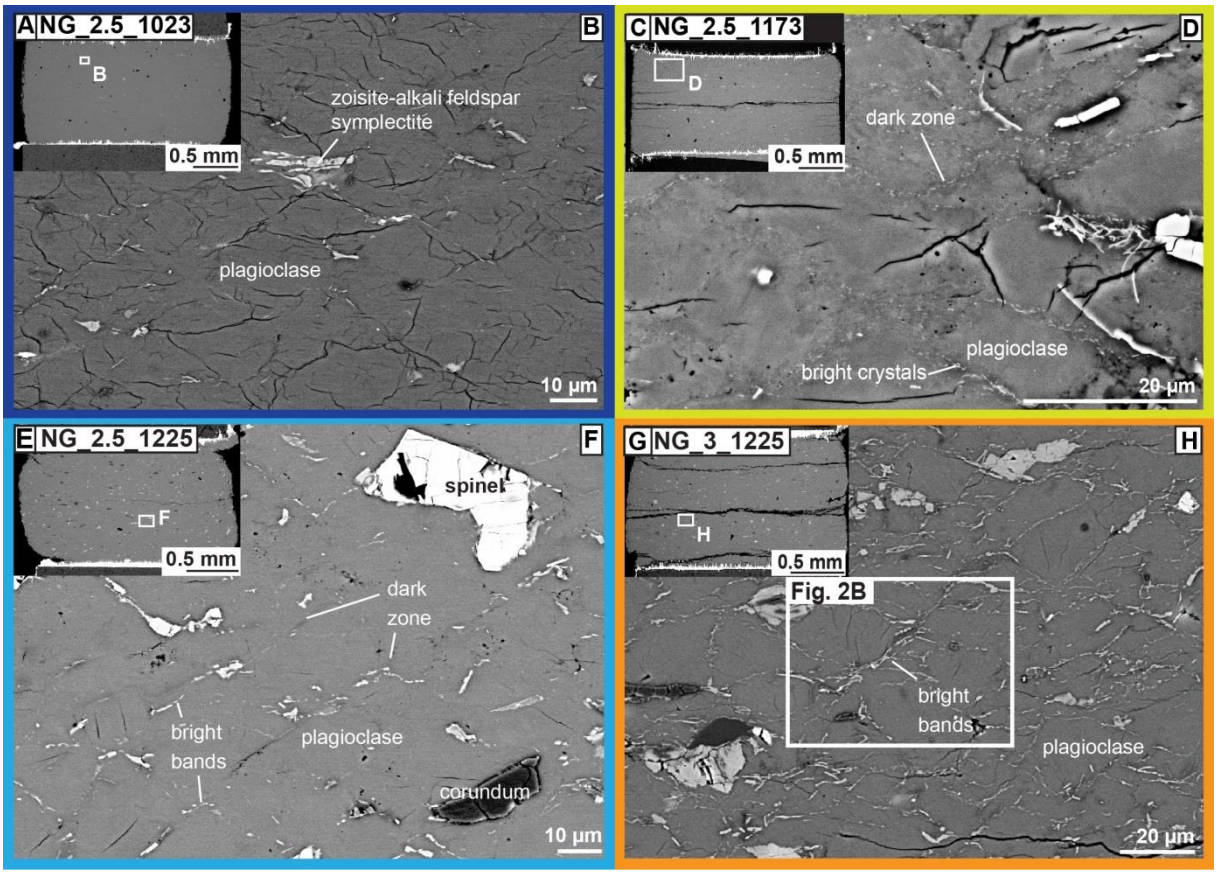

Fig. DR3: Backscattered electron (BSE) images of the four samples after deformation. Compression direction is vertical. The upper-left corner insets show overview images of the entire samples under low magnification (A, C, E, and G). At higher magnification sample NG_2.5_1023 shows distributed microcracks (B). In sample NG_2.5_1173 dark zones mostly contain dark nanocrystals and some brighter ones (D). Sample NG_2.5_1225 reveals dark zones with elongated bright crystals that sometimes form bands (F). The sample NG_3_1225 exhibits almost no dark zones in its microstructure but is completely covered by bright bands (H). The white rectangle in H) marks the location selected for an element distribution map presented in Figure 2B.

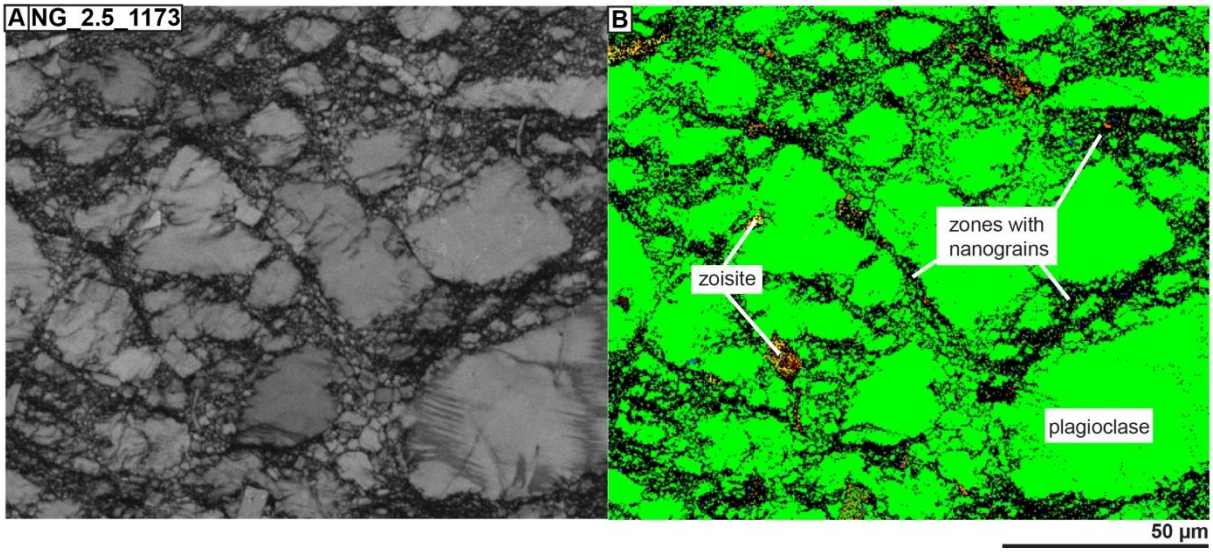

Fig. DR4: Band contrast and phase images of sample NG_2.5_1173. A) The band contrast image demonstrates that the plagioclase matrix is composed of larger plagioclase crystals surrounded by zones filled with crystals that are too small (<0.2 µm) to be identified. B) Phase image of the same area shown in A). Green= plagioclase (bytownite; 70.3 vol. %); orange= zoisite (0.8 vol %); yellow= quartz (0.3 vol %); blue= clinopyroxene (omphacite; 0.7 vol %); dark brown= biotite (0.5 vol %); dark green= garnet (0.1 vol %); black= not identified (27.3 vol. %).

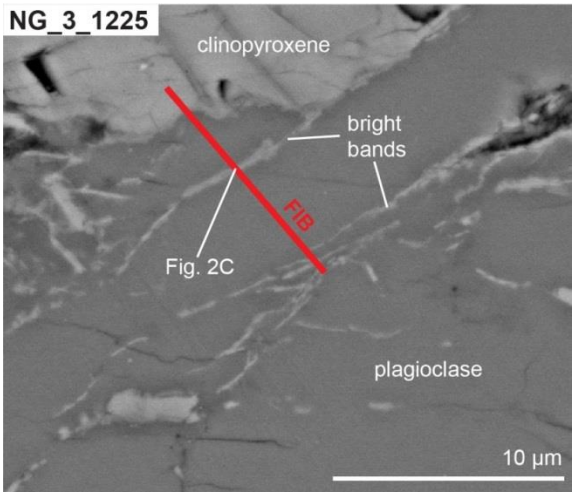

Fig. DR5: Image taken in BSE mode exhibiting the location of the FIB section and the corresponding TEM image shown in Fig. 2C.

Character count: 7,719

Word count: 1,110

Figures and tables: 4

Data Repository: Text and 5 figures. No data housed in a repository or collection outside GSA.

Response to the reviewers

Reviewer #1 (Comments to the Author):

This manuscript presents experimental data that explores the link between the progress of mineral reactions that lead to the conversion of a precursor rock to eclogite and the development of brittle structures. The study appears to be motivated by a widely reported field example from island of Holsnoy in western Norway where granulite facies rocks have been converted to eclogite along discrete structural corridors. The eclogite facies assemblages contain abundant hydrous minerals that have been used by numerous authors as evidence of fluid-assisted reactive conversion of granulite to eclogite. Spatially associated with the eclogite domains are small volumes of pseudotachylite which have been cited by previous studies as evidence of seismicity at eclogite facies conditions. This study is motivated by these previous studies. The experiments in this study use a natural sample obtained from Holsnoy.
The manuscript is well written, and the experiments appear to have been done carefully, and the data is reported in a clear and intelligible way. The overall conclusions are that rates of progress of mineral reactions exert an important control on the formation of brittle structures. In essence, the results are interpreted in two ways. Firstly, in the general case that reaction progress can influence the way in which a rock deforms, and secondly more specifically to the example of Holsnoy. It's the interpretation of the data that I have some concerns about. Perhaps I have misunderstood how the authors are seeking to address the issue of whether earthquakes can be produced by mineral reactions. Implicit in the interpretation of the data is that the acoustic emissions are proxies for seismicity, and by inference are proxies for the formation of pseudotachylite. Because it is the presence of pseudotachyte on Holsnoy that has been used to suggest the existence of deep seated earthquakes and provided the motivation for the presence study. It is these implied links that I'm not convinced of.

Answer #1.1: The record of acoustic emissions is used as a proxy for brittle deformation. While loading a brittle material acoustic emissions reflect the formation of microcracks that eventually grow, coalesce, and eventually lead to brittle failure. Therefore, acoustic emissions also act as precursors prior to macroscopic failure. Hence, acoustic emissions are neither a proxy for seismicity nor can they reflect the formation of pseudotachylytes. In this study we used acoustic emissions to highlight the change in rheological behavior of granulite from dominantly plastic to mostly brittle while undergoing metamorphic transformation at eclogite-facies conditions.

We have also modified the introduction and the concluding paragraphs to clarify that the embrittlement studied here requires the presence of fluids, as in a dry system there will be no reaction. In the Holsnøy case, the initial state of the crust is dry and fluids are introduced by earthquakes. The earthquakes at Holsnøy are interpreted to have formed as aftershocks in a

dry lower crust due to stress pulses generated in the seismogenic regime (Jamtveit et al. 2018) and not by reaction-driven embrittlement. It is the subsequent deformation of the wall rocks after incipient eclogitization that is the part relevant for this study. For the India subduction, however, deep earthquakes are believed to have been triggered by dehydration reactions (Hetényi et al. 2007), and thus in this case reaction-driven embrittlement may also play a role for the earthquake activity in the lower crust.

Perhaps I have misunderstood the results. The authors state that conversion from a plagioclase-rich assemblage to a plagioclase poor assemblage is associated with volume decrease an I guess they are implying that plays an important role in allowing micro fault displacements to be accommodated.

Answer #1.2: Although volume reduction plays an important role in the formation of transformational faults, as previous studies by Stephen Kirby, Pamela Burnley and Harry Green have shown, it is the *reduction of shear strength* due to dynamic recrystallization in the region that undergoes transformation (Kirby, 1987) that is fundamental to accommodate fault slip.

In the experimental realm I think the study is internally consistent, and also appears consistent with previous studies that have investigated similar reaction volume changes, which is good to see.
However, while I realise the experiments may not have been designed specifically to explain the Holsnoy case study, the authors do apply the results to Holsnoy. With regard to Holsnoy, from looking at Bhowany et al (2017) which was referenced as constraining the P-T conditions of the Holsnoy system, I see that Bhowany et al (2017) state that the pseudotachylite-generating brittle deformation predated the formation of the eclogite, and instead the pseudotachytes have recrystallised to plagioclase-rich mineral assemblages. Therefore, I'm unsure how the experiments relate to the Holsnoy system because at face value it appears the Holsnoy rocks had deformed, producing pseudotachylite (and by inference generating earthquakes) before the volume-reducing eclogite reactions had occurred. Therefore, the link between brittle deformation and the progress of metamorphic reactions is circumstantial.

Answer #1.3: The pressure-conditions of the plagioclase bearing assemblage in the recrystallized pseudotachylytes reported by Bhowany et al. was around 1.5 GPa (at ca 680 °C), which for an average crustal density of ca 2.9 g/cm^3 corresponds to a depth of 50-55 km. So even the plagioclase bearing assemblage was formed in the lower crust, and is significantly denser than the original granulite facies assemblage due to abundant new dense phases such as omphacite, zoisite and kyanite. Based on studies of wall rock damage and alteration, it is no doubt that seismic faulting on Holsnøy was synchronous with the formation of a denser assemblage than the original granulites and that the denser assemblages were formed at lower crustal conditions (Austrheim et al., 2017, Science Advances; Petley-Ragan et al., 2018, JGR). Our experiments are also relevant to other examples of deep crustal densification in seismically active areas. Bhowany et al. (2017) point out that the chemical composition of the recrystallized plagioclase changes towards a more Ab-rich plagioclase (Table 4). This indicates that albitization due to anorthite breakdown took place, which is the onset of plagioclase decomposition at higher pressures (Goldsmith, 1981, 1982). Both plagioclase breakdown reactions, anorthite and albite, involve a negative volume change (14-17 %) and

are exothermic (10-13 kJ·mol^{-1}). Our study, in which we observe the breakdown of both components, along with previous studies (Kirby, 1987, Burnley et al. 1990, Kirby et al. 1996), has shown that these thermodynamic characteristics are important to enable embrittlement. To conclude, data show that the conditions of our experiments and the conditions at which eclogitization occurred in Holsnøy can be compared.

I'm not saying the authors are incorrect in their assertion, and as I said above, their experimental data is internally consistent and informative. However to make the work more widely applicable I think the authors should document a series of natural examples that show evidence of brittle deformation the occurred synchronously with metamorphic reactions that have significant deltaV. For example, many granulites show evidence of brittle deformation synchronous with high-grade conditions. If the authors documented examples of reaction inducted micro/meso fracturing, rather than more or less directing their results toward explaining the geological relationships on Holsnoy, I think the manuscript would be more widely applicable.

Answer #1.4: For Holsnøy: Please see answer #1.3. There are also other convincing examples of seismic deformation causally linked to metamorphic reactions associated with a significant volume change, for example in Lofoten, Northern Norway (Menegon et al., 2017, G^3). Also in the Himalayas, there is a correlation between gradual eclogitization of the subducted Indian plate and very deep seismic activity (Hetényi et al., 2007, EPSL).We rewrote the introduction and concluding paragraphs to be more general and present the experiments in the wider context of the eclogitization of the lower crust. In lines 176-186 of the revised manuscript we refer to previous experimental studies (Kirby, 1987; Burnley et al. 1991; Kirby et al. 1996; Incel et al. 2017) on different lithologies that all undergo embrittlement during transformation of a metastable material. They all show similar thermodynamic characteristics.

Several comments

1. Lines 43-44: Agreed, but I don't see the relevance of this statement in this context of this manuscript because you are not talking about deformation at granulite conditions, you are talking about deformation of granulite facies mineral assemblages.

Answer #1.5: The introduction has been changed.

2. Lines 52-55: As I understand it, the field observations show spatial relationship between the formation of eclogite facies mineral assemblages. However from what I can decipher from other studies is that the pseudotachylites predate the eclogite facies mineral assemblages, and therefore what is the direct evidence that that brittle deformation occurred in the deep crust? There are numerous examples of recrystallised pseudotachylite in high-grade rocks. However in each of the cases that I know, the geological history is invariably poly-tectonic, creating ambiguity as to whether pseudotachyte formed toward the end of the first event, or in the early stages of the second event, or at high-grade conditions during the second event. You may well be correct that the pseudotachylites formed at high-grade conditions. However I found a recent paper that you referenced that seemed to suggest that the pseudotachyte recrystallised in plagioclase stable P-T space and were subsequently overprinted by the eclogite mineral assemblages. Therefore what is the unambiguous evidence that brittle

deformation occurred in the deep crust? The description of the geological setting could easily convey to the reader that the granulite and eclogite are somehow geologically related.

Answer #1.6: Please see answers #1.3 and #1.4.

3. I'm confused by the description of starting material and the SEM images. It appears to be a hybrid between the old granulite and a mineral assemblage transitional toward eclogite, with the additional complexity that it has amphibole in it. I'm assuming the amphibole would have formed on the retrograde evolution after rocks reached eclogite? Was the sample chosen specifically to simulate a rock system that had already been infiltrated by fluid? I would have thought a more appropriate starting material might be a sample of pristine granulite with a small amount of experimentally controlled fluid. Although I appreciate determining the amount of fluid might be difficult. Additionally I don't suppose EBSD mapping was undertaken on the material prior to experiments to see if there are relationships between the microstructural character of the samples and their subsequent deformation and metamorphic transformation.

Answer #1.7: We made the choice to work on natural samples so that our results are more relevant to natural systems. We found it very difficult to find a pristine granulite sample that did not show any onset of eclogitization. In most of the granulites we looked at, few zoisite needles and other hydrous phases were present even if the samples were collected at some distance from the pseudotachylyte location. We kept the starting material as 'uneclogitized' as possible by handpicking only plagioclase crystals, but since some zoisite grew into the plagioclase crystals and formed along grain boundaries it was challenging to avoid zoisite in the starting material (Fig. DR1). We did not perform EBSD mappings on the starting material, because we used rock powders that were hot-pressed prior to deformation. Isotropic powders instead of textured natural rocks were used to obtain the powder diffraction pattern that were used to calculate the differential stress evolution during deformation.

Reviewer #2 (Comments to the Author):

The paper by Incel et al represents an important contribution to our understanding of seismicity in the lower crust. Although we know about the granulite-eclogite transition and associated frictional melts in the Bergen Arcs for a long time (probably representing some of the most important geological outcrops in the world), the mechanism for the seismicity remains elusive. Incel et al. have carried out some state-of-the-art experiments to constrain a potential mechanism that couples the metamorphic mineral transformation and the induced seismic faulting. I highly recommend the publication of this article. However, I do have some minor comments that should be taken into consideration prior to publication:

Line 58: What is the reason for saying "may"? Can you upscale or can't you upscale?

Answer #2.1: We changed this sentence to "We show that metamorphic reactions enable embrittlement and propose a model that can be scaled up to natural systems." (lines 49-50).

Line 96: The authors state that the samples furthest away from the plagioclase stability field

produced the least amount of acoustic emission. This is very interesting, but somehow I don't see this picked up later in the text. If it is described it is not clear to me that it links to the statement in line 96. It would be great if the authors could highlight and strengthen this argument.

Answer #2.2: In lines 134-137 of the revised manuscript we refer to this statement with: "If no or little deformation is accommodated by transformation reactions, the granulite is strong and ductile and the microstructure of the sample shows distributed microcracks (Fig. 3A, B), which trigger few acoustic emissions."

Line 97 to 114: The whole paragraph about the microstructural investigation is quite confusing. I highly recommend to clarify this paragraph. For example, in line 99 the authors talk about "appearance of phases". What phases? It comes out of nowhere.

Answer #2.3: We have modified this paragraph and now mention the different phases.

Do you mean mineral phases? Then in line 100, "both features". I understand this refers to the dark areas and "another feature". This needs clarification and more precise wording.

Answer #2.4: We changed the sentence to "Both features, the dark areas and the bright bands, are very small (often <1 µm) and seem to be composed of different phases (Fig. 2B; Fig. DR3D in the Data Repository)." (lines 92-94).

Line 102, "standard analytical techniques"; what are these? Standard is relative, I would call TEM, nanoSIMS, synchrotron nowadays standard. Please be more precise. I assume you can't resolve the chemistry using SEM or microprobe? If so please state this.

Answer #2.5: We changed this paragraph and this sentence has been deleted. We added a new paragraph into the Data Repository about the analytical methods.

Line 104-105: How can you be so sure that Na enriched and Ca depleted is albite or jadeite. Did you balance the the compositions including Si etc or some other ID such as Raman?

Answer #2.6: The newly grown phases are all very small (<0.5 µm). This made it very difficult to obtain precise quantitative analyses. Therefore, we conducted semi-quantitative EDS element distribution maps and compared the results with the chemical composition of the adjacent plagioclase matrix. Since those dark areas, that show enrichment in Na (and also Si) and depletion in Ca relative to the plagioclase matrix, we suggested albite and/or jadeite as possible candidates, because of the available EDS data and due to the fact that one plagioclase breakdown product has to incorporate the released Na.

Line 106-107; This sentence is confusing. You talk about nanocrystalline grains and another phase that is too small to be identified. This (1) reads like as if you have a phase that is smaller than nano and (2) you did TEM so you should know what the "other phase" is.

Answer #2.7: We changed this paragraph and this sentence has been deleted.

Line 109: How do you know that the phases in Fig 2B and C are kyanite and quartz. Again this would benefit from point out what methods was used for mineral ID. I assume SEM/TEM-EDX?

Answer #2.8: Please see answer # 2.5.

Line 110: How did you obtain the chemical composition? Did you do SEM-EDX or TEM-EDX. Some more background is needed here.

Answer #2.9: Please see answer # 2.5. We changed the sentence into “However, energy-dispersive X-ray spectroscopy (EDS) analyses and semi-quantitative element distribution maps were acquired with the scanning electron microscope (SEM) to compare the chemical composition between the plagioclase matrix and these features.” (lines 95-98).

Line 116: Can you point out the "bright bands" in Figure 2?

Answer #2.10: Fig. 2 has been modified to point out the bright bands.

Line 129: I agree with the argumentation about the water source. But have you thought about that the "water" could come from the plagioclase itself? It would be interesting to look at the OH in the plagioclase. Do you have any IR or Raman data on the water content of the plagioclase? Thus could be the faulting be facilitated by a mechanism similar to what Zhang et al. (2004 Nature volume 428, pages 633-63) propose? I feel this should be briefly discussed in the manuscript.

Answer #2.11: We agree and we added the following sentence: “Another possible fluid source could be plagioclase itself since it can contain minor amounts of water in its crystal structure.” (lines 121-122).

Line 135: What is meant with "controlled by the latter process"? This is unclear and should be more precisely worded.

Answer #2.12: We changed the sentence to “It is therefore reasonable to assume that the net rate of eclogitization is controlled by the nucleation and growth of the reaction products.” (lines 128-129).

Methods: I would like to see some more details about the D-DIA experimental setup in the supplements as well as the microscopes used (what SEM/TEM/FIB was used? What were the running conditions?). I assume you did a FIB cut? Where was this cut taken with respect to the material. You show a TEM image in Figure 2c. It would be great to show the cut location in a supplementary figure.

Answer #2.13: Please see answer #2.5. We added a new figure to the Data Repository showing the location for the FIB cut and the position of Fig. 2C. Due to the limited space in Geology, we cannot describe in details the D-DIA setup. We refer to previous studies that used the same technique and we have added the sentence “The experimental setup is explained in detailed in Gasc et al.(2011) and Schubnel et al.(2013).” to the materials and methods paragraph (lines 61-62).

minor comments:

Line 88: There is a lonely bracket at the end of the sentence. Delete or set other bracket.

Answer #2.14: We deleted this lonely bracket.

Line 111: "They are, therefore, interpreted." Please insert comma before and after therefore.

Answer #2.15. This has been corrected.
Line 120: "advanced stage of plagioclase-transformation of 10vol". Try to avoid of...of. Rewording needed.

Answer #2.16: This has been corrected.
Line 142: probably better to say "the microstructure of the sample shows".

Answer #2.17: This has been corrected.
Figure 2: Can you pin-point the TEM image in C in A and B?

Answer #2.18: We added a new figure to the data repository showing the cut location for the FIB section and the position of Fig. 2C.

Reviewer #3:

Relationship between fracturing and reactions. This paper addresses the fundamental point about potential models for development of pseudotachylytes, and implicitly deep crustal earthquakes, under conditions typical of the lower crust. The classic papers by Austrheim and co-workers have clearly demonstrated that fracturing and pseudotachylyte formation is a necessary pre-requisite in order to trigger eclogitization in otherwise dry, strong and metastable granulites (e.g. Austrheim, EPSL 1987; Austrheim's 2013 review paper in Tectonophysics). In other words, there is ample evidence in support of the fact that pseudotachylyte and seismic faulting occurs *before* metamorphic reactions, and triggers them. The present paper tests the hypothesis that metamorphic reactions result in transformational faulting andassociated generation of pseudotachylyte at depth.

This is a viable model, and the experimental results are convincing, but I am not sure that the field relationships in the Bergen Arcs, which the Authors consider as an appropriate natural analogue for their experimental study, can be explained with transformational faulting. The field relationships demonstrate that fracturing occurred prior to metamorphic reactions, and that these reactions are typically localized within pseudotachylyte veins and their damage zone. In the light of this, I would argue that the available observational evidence from key field areas suggests that the "sudden onset of eclogitzation in metastable granulite" (line 57) in nature is triggered by the earthquakes themselves, and not the other way around. The introduction, discussion and conclusions should be modified to better clarify the relationships between fracturing and metamorphic reactions in metastable granulites, as the Authors seem to necessarily invoke alternative mechanisms to brittle fracturing.

Answer #3.1: Please see answer #1.3 to reviewer #1. The initial version of the article was not clear enough on this point and we have modified the introduction and the conclusion. We have added the following sentences in the concluding paragraph "Our results demonstrate that reaction-induced grain size reduction together with a negative volume change trigger embrittlement in the laboratory. This is in accordance with findings of previous numerical and experimental studies on various lithologies (Burnley et al., 1991; Thielmann et al., 2015; Incel et al., 2017) and highlights embrittlement in the lower continental crust, at intermediate depth or deep in Earth's mantle by the same underlying mechanism. It should be noted however,

that the reaction-driven embrittlement mechanism studied here requires a local fluid source. Otherwise, there will be no reaction. In our experiments, there is a small amount of fluid available for hydration reactions. For the Holsnøy case, fluids are introduced to an initially dry lower crust by lower crustal earthquakes. Earthquakes in the lower crust prior to hydration may be triggered through stress pulses from earthquakes in the normal seismogenic regime (i.e. as aftershocks, Jamtveit et al. 2018). Incipient eclogitization reactions would then allow further brittle deformation in the wall rocks of earthquake generated faults. In the case of the subducting Indian lower crust, deep crustal earthquakes have been interpreted to have been triggered by dehydration-produced fluids derived from the crust itself (Hetényi et al., 2007), in which case, reaction-driven embrittlement may even explain the initial earthquake activity." (lines 187-202).

2. Extrapolation to natural conditions. Figure 4 shows the extrapolation of the experimental results to natural conditions, with the implications that the required imposed natural strain rate for transformational faulting are on the order of 10-10 – 10-14.5 s-1. These strain rates are typical of viscous shear zones in nature – although 10-10 s-1 may indicate enhanced creep rates – and are difficult to reconcile with seismic slip velocities. Please clarify how in your model transformational faulting in granulites triggers lower crustal seismicity, if in nature it is expected to occur at the relatively slow strain rates typical of aseismic creep in shear zones. In my view, the experimental results indicate that eclogitization reactions preferentially occur in shear zones rather than in the undeformed granulites. But this brings me back to my first comment. Observational evidence suggests that the nucleation of shear zones in dry and strong granulites requires a brittle precursor, which is typically provided by pseudotachylyte veins, so that earthquakes are necessary to trigger reactions, and not the other way around.

Answer #3.2: Natural strain rates are derived from large-scale deformation data of the entire crust and they do not take into account local strain rate variations due to heterogeneities in chemical composition, grain size, and other factors that influence deformation rates. Therefore, natural strain rates could be locally much higher. Please see also answer #3.1 and #1.3.

Minor comments

Line 45: plastic deformation mechanisms should dominate at granulite facies conditions only in the presence of H2O – see for example the strength envelopes in Jackson et al. (2002) and Bürgmann and Dresen (2008).

Answer #3.3: We changed the sentence to: "On the one hand, previous experimental studies revealed that plastic deformation should be dominant in plagioclase-rich rocks under granulite-facies conditions (<1 GPa and 973 K; Tullis and Yund, 1992) in the presence of water (Bürgmann and Dresen, 2008)." (lines 40-42).

Lines 45-48: as a follow-up comment, the brittle-viscous transition of dry plagioclase-rich rocks is expected to occur at depth in excess of 20-30 km, so that frictional (and co-seismic) slip under high differential stress can be expected in effectively dry granulites (e.g. see also Bodin & Horton, BSSA 94, 2004). See also my main comment 1 above.

Answer #3.4: The introduction has been modified.

Lines 51: grain size reduction by which mechanism?

Answer #3.5: The introduction has been modified and this sentence has been removed.

Line 90: please add the stress-strain curves (your figure DR2) to Fig. 1. These are very important data that should be included in the paper.

Answer #3.6: Unfortunately, due to the length limitations for an article in Geology we are neither able to add this figure to the main text nor to figure 1.

Lines 120 (and Table 1): please specify how you have estimated the degree of eclogitization. By image analysis of the area fraction of the reaction products?

Answer #3.7: We added the sentence "Reaction progress was estimated based on image analysis of the area fraction of the reaction products. " (lines 114-115).

Line 214: Please add labels with the sample number and the experiment type (weak/ductile, brittle, strong/ductile) to the images in A-C.

Answer #3.8: We added those labels to Fig. 2.

Line 215: replace "composite image" with "composite EDS elemental map"; I cannot see the location of Fig. 2C in Fig. DR3H.

Answer #3.9: We added EDS and we added a figure into the data repository showing the location of Fig. 2C.

Line 228: please discuss possible reasons for NG_2.5_1225 to be brittle despite the high amount of eclogitization.

Answer #3.10: We changed the sentence to "Although the net eclogitization rate in sample NG_2.5_1225 is higher compared to sample NG_2.5_1173, this sample is also brittle (E, F), because the amount of soft eclogite is not sufficient to dominate the overall rheological behavior." to the caption (lines 222-225).

Fig. DR4: please provide details of the EBSD analysis (SEM type, acquisition software and conditions, processing routine). The phase map in Fig. DR4B shows four colours: green is plagioclase, but please specify which phases are coloured in yellow, red and blue.

Answer #3.11: Details on the analytical methods were added into the Data Repository and different phases shown in Fig DR4B are now specified.